

Formation of TiO₂ Nanopores by Anodization of Ti-Films

Patricia M. Perillo*, Daniel F. Rodríguez

National Atomic Energy Commission, CAC, Buenos Aires, Argentina
Email: perillo@cnea.gov.ar

Received 2 May 2014; revised 5 June 2014; accepted 17 June 2014

Copyright © 2014 by authors and OALib.

This work is licensed under the Creative Commons Attribution International License (CC BY).

<http://creativecommons.org/licenses/by/4.0/>



Open Access

Abstract

Titania nanopores were fabricated on silicon substrate. Ti thin films (600 nm) were first deposited by radio-frequency (RF) magnetron sputtering at two substrate temperatures and then anodized in glycerol electrolytes containing NH₄F. The morphology and structure were identified by means of scanning electron microscopy (SEM), X-ray diffractometry (XRD). The effect of the temperature on the Ti thin films deposited by RF magnetron sputtering and the applied voltage on nanopore morphology were investigated. Homogeneously distributed nanopores with dimensions in the range of 60 to 80 nm were obtained independently of the voltage applied during the anodization and the substrate temperature in sputtering deposition.

Keywords

RF Magnetron Sputtering, TiO₂, Nanopores, Anodic Oxidation

Subject Areas: Electrochemistry, Nanometer Materials, Surface and Intersurface of Materials

1. Introduction

Highly ordered, vertically oriented TiO₂ nanotube-arrays fabricated by potentiostatic anodization of titanium constitute a material architecture that offers a large internal surface area. TiO₂ nanotube arrays have been found to possess a variety of advanced applications, including their use in sensors [1]-[7], dye sensitized solar cells [8]-[10], hydrogen generation by water photoelectrolysis [11], photocatalytic reduction of CO₂ under outdoor sunlight [12], and supercapacitors [13] [14].

Nanotubes arrays also have proved useful in related biomedical applications including molecular filtration, biosensors, tissue engineering and drug delivery [15]-[17].

*Corresponding author.

However, most of the works have been focused on the anodization of titanium foils, which limits the application of such a material in functional microdevices (e.g. dye-sensitized solar cells or electrochromic devices) [18] [19]. It is therefore desirable to develop processes that facilitate the manufacture of TiO₂ nanotubes or nanopores on an adequate substrate before electrochemical anodization. In recent years, some researchers have used the electrochemical anodization method to successfully grow the nanotube arrays from thin titanium films on a variety of substrates including glass [20]-[22], conducting glass (FTO, ITO) [21] [23], and silicon [24]-[27]. Ti thin films deposited on a semiconductor substrate, such as p-type Si (100), which has many promising applications in the development of future electronic devices. However, there are very few reports about the comprehensive research on the influence of the titanium thin films microstructure on the growth of anodic TiO₂.

We have successfully developed films via anodizing metal titanium thin films deposited by RF magnetron sputtering on silicon substrates. Therefore, in this paper, we will discuss the effects of the microstructure of Ti films on the growth of TiO₂ nanotube or nanopore, in order to optimize the fabrication process and finally to improve their properties. The effect of the temperature on the Ti thin films and the applied voltage on nanopore morphology were investigated.

2. Experimental Procedure

2.1. Deposition of a Ti Thin Film on a Si Substrate

Ti films (600 nm in thickness) were deposited by RF magnetron sputtering on p-type Si (100) wafer with 300 nm layer of SiO₂ at room temperature in some cases and at 500°C in another. Target of 99.9% Ti was used as the material source. The chamber pressure was maintained at 0.5 Pa during the deposition process. Sputtering was carried with a pure gas argon flowing of 8 cm³/min. The distance between the target and the substrate was 14 cm and the sputtering power was 150 W using RF power supply. Under these conditions, the deposition rate was 2.9 nm/min and a 600 nm thick Ti film was obtained after 210 min.

2.2. Fabrication of TiO₂ Nanostructure

Prior to the experiments the Si samples were degreased by sonicating in acetone, isopropanol and rinsed with deionized water (DI) and dried in a nitrogen stream.

Anodization was performed applying a ramp during 30 min from 0 to the desire voltage (20, 60, 80, 100 V) and finally holding the voltage constant during for 1 h using a Keithley 6517B electrometer. The growth of the nanotube or nanopore arrays has been obtained in a glycerol solution with 0.6% ammonium fluoride in an electrochemical cell with a platinum foil (1 cm²) as cathode and titanium film as anode at room temperature. Current variation during a nodizing was simultaneously monitored by a Keithley 2000 multimeter. The solution was stirred [28] using a magnetic stirring bar (20 mm long) at 150 rpm (referred as SAT). The distance between the two electrodes was kept at 2 cm in all the experiments. After the electrochemical treatment, the specimens were rinsed with deionized water and dried with a nitrogen stream. The anodized TiO₂ was annealed to develop the anatase TiO₂ nanostructure at 550°C for 120 min in air.

2.3. Characterization of TiO₂ on Ti Thin Film

The samples of the Ti film and TiO₂ were characterized by scanning electron microscopy (SEM), X-ray diffraction (XRD). Scanning electron microscopes (Fei model Quanta 200 and Zeiss Supra40 Gemini) were employed for the morphological characterization of the TiO₂ samples. X-ray diffraction (XRD) patterns were recorded with a diffractometer (PANalytical model Empyrean) equipped Cu K α ($\lambda = 0.15418$ nm) using a generator voltage of 40 kV and current of 40 mA.

3. Results and Discussion

3.1. Effect of Sputtering Parameters on Microstructure of Titanium Films

The effect of the substrate temperature on the microstructural morphologies of titanium film deposited by RF magnetron sputtering technique was investigated. The morphology of thin films deposited by sputtering depends of the ratio of the substrate temperature (T_s) to the melting point of the film (T_m), therefore T_s/T_m . When $T_s/T_m < 0.3$ the morphology of the film consists of columns typically tens of nanometers in diameter with an a few nm

inter-columnar zone that separates them. The columns have poor crystallinity or are amorphous. However if $T_s/T_m > 0.3$ the morphology of the film results in more isotropic and equiaxed crystallite shapes [26] [29].

With a substrate at room temperature ($T_s \approx 25^\circ\text{C}$) to Ti fusion ($T_m = 1660^\circ\text{C}$) temperature (T_s/T_m) ratio of 0.02 indicates that the surface morphology of Ti films should be in accordance with columnar structures. Nevertheless with 500°C the substrate temperature the ratio is 0.3 therefore hoping for an equiaxed crystallite shapes.

Figure 1 shows the SEM top images of Ti films deposited by RF magnetron sputtering at room temperature and 500°C . Both films have fine granular structure, but more rough and some Ti grain coarse at 500°C it was observed. From the morphological analysis carried out using observation by SEM, the grain size was calculated in all samples. The grain size of films deposited at room temperature was 60 nm and 80 nm at 500°C . The roughness of arithmetical mean deviation was measured by atomic force microscope (AFM) obtaining 14 nm at room temperature and 88 nm at 500°C , respectively. With the increase of the substrate temperature, the atoms migrate from the surface, the denseness is improved and grows a crystalline structure [30]. In titanium film deposited at high temperature a good film adhesion was observed. Heated silicon substrate could improve the denseness and crystallinity of the films, and also make Ti grains coarsen.

In **Figure 2**, XRD patterns of Ti deposited by RF magnetron sputtering at room temperature and 500°C were shown. Typical peaks of titanium phase at 2θ near 35° , 38° and 40° are observed in the XRD pattern which correspond to the planes (100), (002) and (101), respectively. All of peaks are identified as hexagonal Ti (00-044-1294).

The strongest peak for the room temperature sample consists to (100) titanium, which is its preferential orientation during the sputtering process (**Figure 2(a)**). However, with the increase in the substrate temperature no preferred orientation is observed. The ratio of the peaks is similar as Ti (00-044-1294) card (**Figure 2(b)**).

The competition between energy and surface free energy affecting the textures of the grains are heavily depend on the different parameters such as substrate temperature, pressure, power and substrate properties. The (100), (101) or (002) orientations are the preferable ones in Ti films depending on the parameters mentioned above [31]-[34].

The XRD results of the Ti films with varying substrate temperature may be interpreted on the basis of stress and the strain evolution mechanism. The compressive stress induced in the films contributed to the development of (100) orientation and it may have relaxed to tensile mode at higher substrate temperature favoring the equiaxed orientation.

The lattice parameter was calculated by equaling the interplanar spacing d obtained from the position of the (100) peak using the Bragg condition. The values of lattice parameters are summarized in **Table 1**. The strain along the a-axis, α is given by the following eq. $\alpha = (a - a_0)/a_0 \times 100$ where a is the lattice parameter of the strained Ti film calculated from XRD data and a_0 is the unstrained lattice parameter [32].

The value of strain was found negative in the case of 25°C substrate temperature with a corresponding change in crystallite size from 2.95 to 2.90. However in the case of 500°C substrate temperature the value of strain was found negligible. It shows the influence temperature on the microstrain of the Ti thin film.

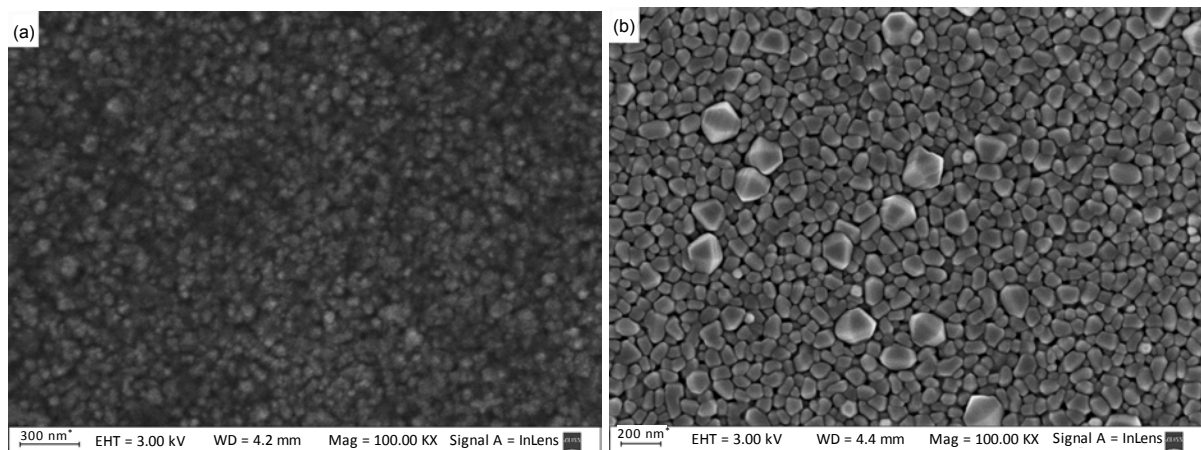


Figure 1. SEM top views of Ti films deposited at a) room temperature b) 500°C .

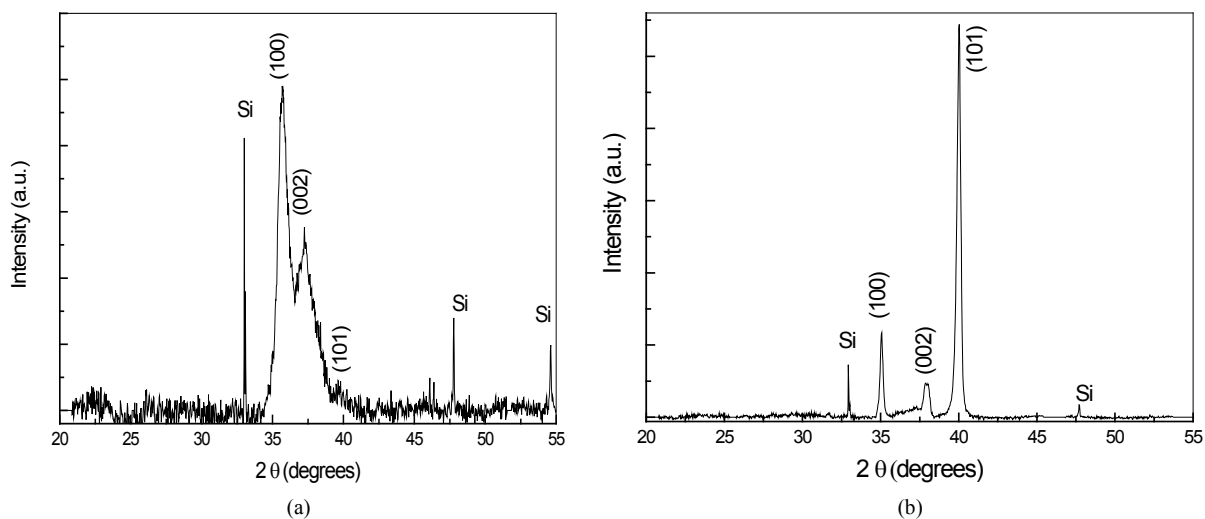


Figure 2. XRD patterns of Ti films deposited at a) room temperature b) 500°C.

Table 1. Influence of substrate temperature on the microstrain, roughness and grain size of the Ti thin.

Parameters	Grain size (nm)	Average roughness (nm)	Lattice arameter (Å)	Microstrain (100) peak
25°C	60	14	2.901	-1.69
500°C	80	88	2.955	0.14

The microstrain (100) peak in the case of 25°C substrate temperature is compressive in nature and it decreases with the increase of temperature. The above is compatible with the thermal stress appearing on silicon by depositing titanium [35]. Moreover when Ti thin film is deposited on large mismatch substrate like glass, the (002) orientation is the preferable [33]. The reason may be attributed to the fact that the different surface free energies are associated with different planes [36].

In our case the different thermal expansion coefficient between Ti and substrate gives then rises to compressive stresses in the film. The thermal stress induced in the thin film may have also contributed to determine the preferred orientation (100) in Ti film deposited at room substrate temperature.

3.2. TiO₂ Nanostructure Thin Films

Figure 3 shows the SEM image of anodic TiO₂ fabricated from Ti film deposited on Si substrate at room temperature and 500°C and different voltages (20, 60, 80 and 100 V). In order to convert the amorphous TiO₂ structure into a crystalline one, samples were annealed at 550°C for 2 h in air.

Figures 3(a)-(d) show the anodized TiO₂ formed for the case of titanium deposited at room temperature at 20, 60, 80 and 100 V, respectively. Moreover in **Figures 3(e)-(h)** show the TiO₂ formed for the case of titanium deposited at 500°C at 20, 60, 80 and 100 V, respectively.

In **Figures 3(a)-(d)** it can be seen a nanoporous structure but **Figures 3(e)-(h)** show a more uniform structure. There are some grains with sizes well above the average. In these grains grow over one nanopore. The diameter of the pore remain relatively constant independently the applied voltage.

Figure 4 shows the size of nanostructure grown on Ti films deposited at room temperature and 500°C as a function of the applied voltage. The nanostructure size is approximately 60 nm in all cases. In this work, we obtained a Ti film with very small grain size, less than 100 nm. Therefore the nanostructure size may be limited by the grain size of the deposited titanium film and not to the applied voltage in the anodization. However according to the literature in the case of Ti sheet, it is well known that with increasing potential the size diameter always increases, this is in line with growth of anodic compact oxides. The grain size in Ti sheet is in the order of microns, therefore is not conditioning for the growth of the nanostructure in the anodization process.

In the case of Ti thin films using conventional deposition methods, is possible to obtain by anodization different microstructures like nanopores or nanotubes [27] [31]. According to the technique used and the parameters in which deposition takes place (temperature, pressure, power) is possible to obtain Ti thin films with different

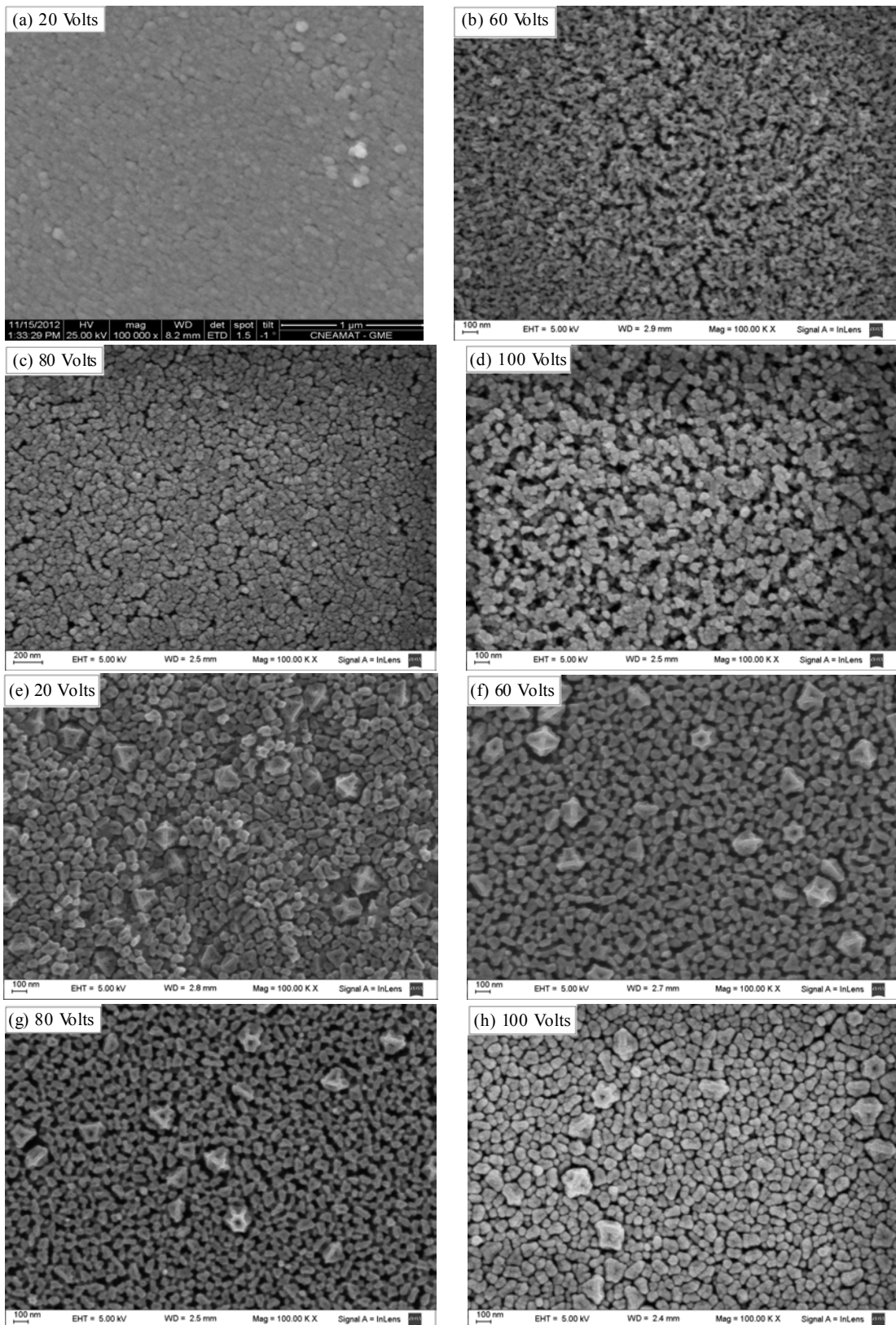


Figure 3. SEM top images of TiO_2 structure formed by anodization of Ti films deposited at a) b) c) d) room temperature and e) f) g) h) 500°C .

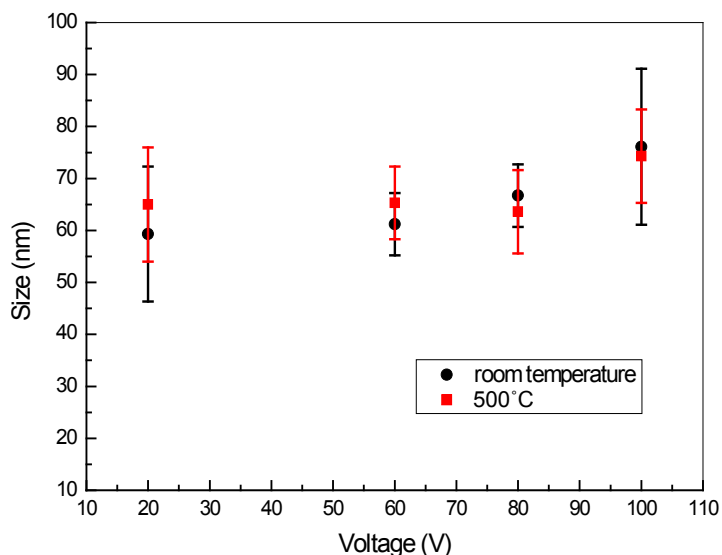


Figure 4. Size of TiO₂ nanostructure grown on Ti films deposited at room temperature and 500°C as a function of the applied voltage.

grain size, roughness and crystal orientation.

It is well known that the TiO₂ nanostructures grown by anodization strongly depend off the morphology of the Ti film deposited on substrate. Some authors claim that the columnar structure in Ti thin film is essential for the nanotubes formation by anodic oxidation [26]. Other ones affirm that the crystallographic orientation of the Ti thin film is critical for the nanotubes obtention, but there have been cases in which the Ti thin film structure was columnar and nanopores were obtained instead of nanotubes. As well it was reported the growth of nanotubes from Ti thin film with different crystallographic orientation [31]. Others said that a possible cause for the formation of pores versus tubes could have been roughness differences [37]. An additional factor for pore and tube growth is associated with the presence of F⁻ ions in the electrolyte and dissolution of metal-fluoride complexes [38].

In summary the experimental details of the anodization process and the metal surface conditions strongly influence the growth of nanoporous/nanotubular structures.

The corresponding XRD patterns of TiO₂ nanopores fabricated from Ti film deposited on Si substrate at room temperature and 500°C after being annealed are shown in **Figure 5**. The structure evidently consists of a mixed phase of anatase (01-086-1157) and rutile (00-034-0180). According with the literature it is well known that there are a mixture of phases which depend strongly on heat treatment [39] [40] and of the substrate temperature during the deposition of the film [41].

Typical peaks of anatase phase at 2θ near 25°, 37° and 48° are observed in the XRD pattern, which correspond to planes (101), (004) and (200), respectively and typical peaks of rutile phase at 2θ near 27°, 36°, 41° and 54° are observed in the XRD pattern which correspond to the planes (110), (101), (111) and (211), respectively.

At room temperature the strongest peak correspond to anatase phase (**Figure 5(a)**), while at 500°C there are similar peaks corresponding to anatase and rutile phases (**Figure 5(b)**). The peak at 2θ near 33° belongs to Si (200) plane of the substrate. These results show that substrate temperature during titanium deposition influence strongly in the crystal structure of TiO₂ nanotubes obtained by anodizing. The crystallinity degree of the rutile phase increases by increasing substrate temperature.

4. Conclusions

Ti films deposited by RF magnetron sputtering at room substrate temperature and 500°C were performed on silicon substrate. Nanoporous titanium oxide film was prepared by the anodization of titanium films in a glycerol solution with 0.6% ammonium fluoride at room temperature. In order to convert the amorphous TiO₂ structure into a crystalline one, samples were annealed at 550°C for 2 h in air.

The nanoporous titanium oxide films had homogeneously distributed pores with an average pore diameter of

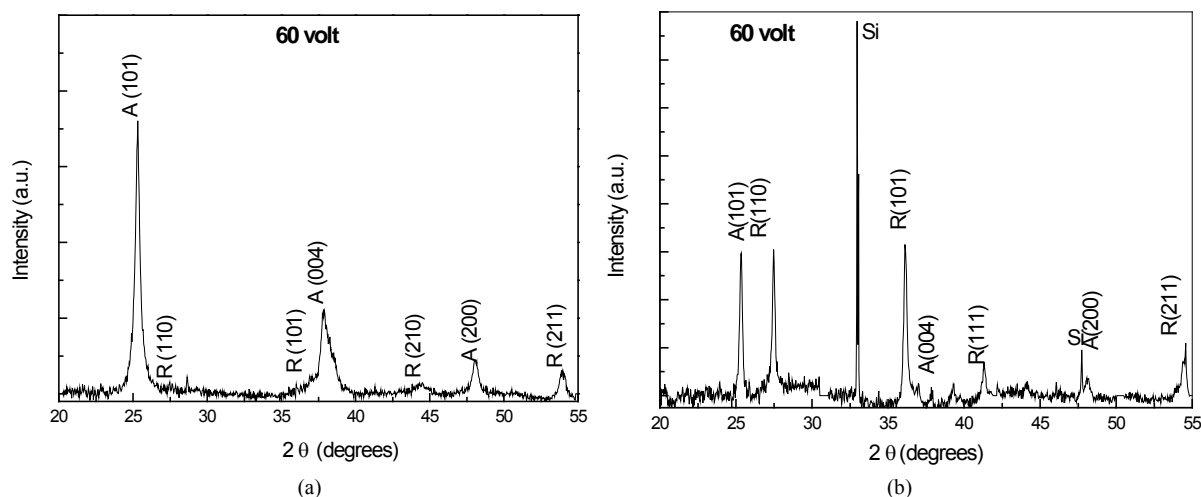


Figure 5. XRD patterns of TiO₂ nanostructure prepared on Ti films at a) room temperature b) 500°C.

60 nm independently of the voltage applied and the substrate temperature in sputtering deposition. Probably the pore size is limited by the grain size of the deposited titanium and not by the preferred orientation of the thin film titanium.

In summary, a possibly critical parameter for the grow of the nanostructure is the grain size of the titanium thin film. If the grain size is very small, the pore diameter does not depend on the voltage applied during the anodization process.

Further investigation is required to understand the relationship between the formation nanotubes/nanopores and the microstructure of Ti thin film.

References

- [1] Mor, G.K., Carvalho, M.A., Varghese, O.K., Pishko, M.V. and Grimes C.A. (2004) A Room Temperature TiO₂ Nanotube Hydrogen Sensor Able to Self-Clean Photoactively from Environmental Contamination. *Journal of Materials Research*, **19**, 628-634. <http://dx.doi.org/10.1557/jmr.2004.19.2.628>
- [2] Varghese, O.K., Mor, G.K., Grimes, C.A., Paulose, M. and Mukherjee, N. (2004) A Titania Nanotube-Array Room-Temperature Sensor for Selective Detection of Hydrogen at Low Concentrations. *Journal of Nanoscience and Nanotechnology*, **4**, 733-737. <http://dx.doi.org/10.1166/jnn.2004.092>
- [3] Paulose, M., Varghese, O.K., Mor, G.K., Grimes, C.A. and Ong, K.G. (2006) Unprecedented Ultra-High Hydrogen Gas Sensitivity in Undoped Titania Nanotubes. *Nanotechnology*, **17**, 398-402. <http://dx.doi.org/10.1088/0957-4484/17/2/009>
- [4] Varghese, O.K., Yang, X., Kendig, J., Paulose, M., Zeng, K., Palmer, C., Ong, K.G. and Grimes, C.A. (2006) A Transcutaneous Hydrogen Sensor: From Design to Application. *Sensor Letters*, **4**, 120-128. <http://dx.doi.org/10.1166/sl.2006.022>
- [5] Varghese, O.K., Gong, D., Paulose, M., Ong, K.G., Dickey, E.C. and Grimes, C.A. (2003) Extreme Changes in the Electrical Resistance of Titania Nanotubes with Hydrogen Exposure. *Advanced Materials*, **15**, 624-627. <http://dx.doi.org/10.1002/adma.200304586>
- [6] Sxennik, E., Colak, Z., Kılınc, N. and Ziya Oüturk, Z. (2010) Synthesis of Highly-Ordered TiO₂ Nanotubes for a Hydrogen Sensor. *International Journal of Hydrogen Energy*, **35**, 4420-4427. <http://dx.doi.org/10.1016/j.ijhydene.2010.01.100>
- [7] Wang, Q., Pan, Y.Z., Huang, S.S., Ren, S.T., Li, P. and Li, J.J. (2011) Resistive and Capacitive Response of Nitrogen-Doped TiO₂ Nanotubes Film Humidity Sensor. *Nanotechnology*, **22**, Article ID: 025501. <http://dx.doi.org/10.1088/0957-4484/22/2/025501>
- [8] Shankar, K., Mor, G.K., Prakasam, H.E., Yoriya, S., Paulose, M., Varghese, O.K. and Grimes, C.A. (2007) Highly-Ordered TiO₂ Nanotube Arrays up to 220 μm in Length: Use in Water Photoelectrolysis and Dye-Sensitized Solar Cells. *Nanotechnology*, **18**, Article ID: 065707. <http://dx.doi.org/10.1088/0957-4484/18/6/065707>
- [9] Macák, J.M., Tsuchiya, H., Ghicov, A. and Schmuki, P. (2005) Dye-Sensitized Anodic TiO₂ Nanotubes. *Electrochemistry Communications*, **7**, 1133-1137. <http://dx.doi.org/10.1016/j.elecom.2005.08.013>

- [10] Adachi, M., Murata, Y., Okada, I. and Yoshikawa, Y. (2003) Formation of Titania Nanotubes and Applications for Dye-Sensitized Solar Cells. *Journal of the Electrochemical Society*, **150**, G488-G493. <http://dx.doi.org/10.1149/1.1589763>
- [11] Mohapatra, S.K., Misra, M., Mahajan, V.K. and Raja, K.S. (2007) Design of a Highly Efficient Photoelectrolytic Cell for Hydrogen Generation by Water Splitting: Application of TiO₂-C Nanotubes as a Photoanode and Pt/TiO₂ Nanotubes as a Cathode. *Journal of Physical Chemistry C*, **111**, 8677-8685. <http://dx.doi.org/10.1021/jp071906v>
- [12] Varghese, O.K., Paulose, M. and LaTempa, T.J. (2009) High-Rate Solar Photocatalytic Conversion of CO₂ and Water Vapor to Hydrocarbon Fuel. *Nano Letters*, **9**, 731-737. <http://dx.doi.org/10.1021/nl803258p>
- [13] Wang, Y.G., Wang, Z.D. and Xia, Y.Y. (2005) An Asymmetric Supercapacitor Using RuO₂/TiO₂ Nanotube Composite and Activated Carbon Electrodes. *Electrochimica Acta*, **50**, 5641-5646. <http://dx.doi.org/10.1016/j.electacta.2005.03.042>
- [14] Wang, Q., Wen, Z.H. and Li, J.H. (2007) Carbon Nanotubes/TiO₂ Nanotubes Hybrid Supercapacitor. *Journal of Nanoscience and Nanotechnology*, **7**, 3328-3331. <http://dx.doi.org/10.1166/jnn.2007.679>
- [15] Oh, S., Daraio, C., Chen, L.-H., Pisanic, T.R., Fiñones, R.R. and Jin, S. (2006) Significantly Accelerated Osteoblast Cell Growth on Aligned TiO₂ Nanotubes. *Journal of Biomedical Materials Research Part A*, **78A**, 97-103. <http://dx.doi.org/10.1002/jbm.a.30722>
- [16] Papat, K.C., Eltgroth, M., La Tempa, T.J., Grimes, C.A. and Desai, T.A. (2007) Decreased *Staphylococcus epidermis* Adhesion and Increased Osteoblast Functionality on Antibiotic-Loaded Titania Nanotubes. *Biomaterials*, **28**, 4880-4888. <http://dx.doi.org/10.1016/j.biomaterials.2007.07.037>
- [17] Roy, S.C., Paulose, M. and Grimes, C.A. (2007) The Effect of TiO₂ Nanotubes in the Enhancement of Blood Clotting for the Control of Hemorrhage. *Biomaterials*, **28**, 4667-4672. <http://dx.doi.org/10.1016/j.biomaterials.2007.07.045>
- [18] Mor, G.K., Shankar, K., Paulose, M., Varghese, O.K. and Grimes, C.A. (2006) Use of Highly-Ordered TiO₂ Nanotube Arrays in Dye-Sensitized Solar Cells. *Nano Letters*, **6**, 215-218. <http://dx.doi.org/10.1021/nl052099j>
- [19] Paulose, M., Shankar, K., Varghese, O.K., Mor, G.K. and Grimes, C.A. (2006) Application of Highly-Ordered TiO₂ Nanotube-Arrays in Heterojunction Dye-Sensitized Solar Cells. *Journal of Physics D: Applied Physics*, **39**, 2498-2503. <http://dx.doi.org/10.1088/0022-3727/39/12/005>
- [20] Mor, G.K., Varghese, O.K., Paulose, M. and Grimes, C.A. (2005) Transparent Highly Ordered TiO₂ Nanotube Arrays via Anodization of Titanium Thin Films. *Advanced Functional Materials*, **15**, 1291-1296. <http://dx.doi.org/10.1002/adfm.200500096>
- [21] Leenheer, A.J., Miedaner, A., Curtis, C.J., Van Hest, M.F.A.M. and Ginley, D.S. (2007) Fabrication of Nanoporous Titania on Glass and Transparent Conducting Oxide Substrates by Anodization of Titanium Films. *Journal of Materials Research*, **22**, 681-687. <http://dx.doi.org/10.1557/jmr.2007.0078>
- [22] Chu, S.Z., Inoue, S., Wada, K., Hishita, S. and Kurashima, K. (2005) Self-Organized Nanoporous Anodic Titania Films and Ordered Titania Nanodots/Nanorods on Glass. *Advanced Functional Materials*, **15**, 1343-1349. <http://dx.doi.org/10.1002/adfm.200400253>
- [23] Sadek, A.Z., Zheng, H., Latham, K., Wlodarski, W. and Kalantar-zadeh, K. (2009) Anodization of Ti Thin Film Deposited on ITO. *Langmuir*, **25**, 509-514. <http://dx.doi.org/10.1021/la802456r>
- [24] Yu, X.F., Lu, Y.X., Wlodarski, W., Kandasamy, S. and Kalantar-zadeh, K. (2008) Fabrication of Nanostructured TiO₂ by Anodization: A Comparison between Electrolytes and Substrates. *Sensors and Actuators B*, **130**, 25-31. <http://dx.doi.org/10.1016/j.snb.2007.07.076>
- [25] Macák, J.M., Tsuchiya, H., Berger, S., Bauer, S., Fujimoto, S. and Schmuki, P. (2006) On Wafer TiO₂ Nanotube-Layer Formation by Anodization of Ti-Films on Si. *Chemical Physics Letters*, **428**, 421-425. <http://dx.doi.org/10.1016/j.cplett.2006.07.062>
- [26] Premchand, Y.D., Djenizian, T., Vacandio, F. and Knauth, P. (2006) Fabrication of Self-Organized TiO₂ Nanotubes from Columnar Titanium Thin Films Sputtered on Semiconductor Surfaces. *Electrochemistry Communications*, **8**, 1840-1844. <http://dx.doi.org/10.1016/j.elecom.2006.08.028>
- [27] Yu, X.F., Li, Y.X., Ge, W., Yang, Q., Zhu, N.F. and Kalantar-zadeh, K. (2006) Formation of Nanoporous Titanium Oxide Films on Silicon Substrates Using an Anodization Process. *Nanotechnology*, **17**, 808-814. <http://dx.doi.org/10.1088/0957-4484/17/3/033>
- [28] Patermarakis, G. and Moussoutzanis, K. (1995) Mathematical Models for the Anodization Conditions and Structural Features of Porous Anodic Al₂O₃ Films on Aluminum. *Journal of the Electrochemical Society*, **142**, 737-743. <http://dx.doi.org/10.1149/1.2048527>
- [29] Lackner, J.M., Waldhauser, W., Alamanou, A., Teichert, C., Schmied, F., Major, L. and Major, B. (2010) Mechanisms for Self-Assembling Topography Formation in Low-Temperature Vacuum Deposition of Inorganic Coatings on Polymer Surfaces. *Bulletin of the Polish Academy of Sciences*, **58**, 281-294.

- [30] Mor, G.K., Varghese, O.K., Paulose, M. and Grimes, C.A. (2005) Transparent Highly Ordered TiO₂ Nanotube Arrays via Anodization of Titanium Thin Films. *Advanced Functional Materials*, **15**, 1291-1296. <http://dx.doi.org/10.1002/adfm.200500096>
- [31] Kalantar-zadeh, K., Sadek, A.Z., Zheng, H., Partridge, J.G., McCulloch, D.G., Li, Y.X., Yu, X.F. and Wlodarski, W. (2009) Effect of Crystallographic Orientation on the Anodic Formation of Nanoscale Pores/Tubes in TiO₂ Films. *Applied Surface Science*, **256**, 120-123. <http://dx.doi.org/10.1016/j.apsusc.2009.07.088>
- [32] Chawla, V., Jayaganthan, R., Chawla, A.K. and Chandra, R. (2009) Microstructural Characterizations of Magnetron Sputtered Ti Films on Glass Substrate. *Journal of Materials Processing Technology*, **209**, 3444-3451. <http://dx.doi.org/10.1016/j.jmatprotec.2008.08.004>
- [33] Jeyachandran, Y.L., Karunakaran, B., Narayandass, S.K., Mangalaraj, D., Jenkins, T.E. and Martin, P.J. (2006) Properties of Titanium Thin Films Deposited by dc Magnetron Sputtering. *Materials Science and Engineering: A*, **431**, 277-284. <http://dx.doi.org/10.1016/j.msea.2006.06.020>
- [34] Oya, T. and Kusano, E. (2009) Effects of Radio-Frequency Plasma on Structure and Properties in Ti Film Deposition by dc and Pulsed dc Magnetron Sputtering. *Thin Solid Films*, **517**, 5837-5843. <http://dx.doi.org/10.1016/j.tsf.2009.03.055>
- [35] Chawla, V., Jayaganthan, R. and Chandra, R. (2008) Finite Element Analysis of Thermal Stress in Magnetron Sputtered Ti Coating. *Journal of Materials Processing Technology*, **200**, 205-211. <http://dx.doi.org/10.1016/j.jmatprotec.2007.09.036>
- [36] Singh, P. and Kaur, D. (2008) Influence of Film Thickness on Texture and Electrical Properties of Room Temperature Deposited Nanocrystalline V₂O₅ Thin Films. *Journal of Applied Physics*, **103**, Article ID: 043507. <http://dx.doi.org/10.1063/1.2844438>
- [37] Kalantar-zadeh, K., Sadek, A.Z., Partridge, J.G., McCulloch, D.G., Li, Y.X., Yu, X.F., Spizirri, P.G. and Wlodarski, W. (2009) Nanoporous Titanium Oxide Synthesized from Anodized Filtered Cathodic Vacuum Arc Ti Thin Films. *Thin Solid Films*, **518**, 1180-1184. <http://dx.doi.org/10.1016/j.tsf.2009.03.223>
- [38] Kowalski, D., Kim, D. and Schmuki, P. (2013) TiO₂ Nanotubes, Nanochannels and Mesosponge: Self-Organized Formation and Applications. *Nano Today*, **8**, 235-264. <http://dx.doi.org/10.1016/j.nantod.2013.04.010>
- [39] Macák, J.M., Aldabergerova, S., Ghicov, A. and Schmuki, P. (2006) Smooth Anodic TiO₂ Nanotubes: Annealing and Structure. *Physica Status Solidi (a)*, **203**, 67-69. <http://dx.doi.org/10.1002/pssa.200622214>
- [40] Regonini, D., Jaroenworarluck, A., Stevens, R. and Bowen, C.R. (2010) Effect of Heat Treatment on the Properties and Structure of TiO₂ Nanotubes: Phase Composition and Chemical Composition. *Surface and Interface Analysis*, **42**, 139-144. <http://dx.doi.org/10.1002/sia.3183>
- [41] Ben Amor, S., Guedri, L., Baud, G., Jacquet, M. and Ghedira, M. (2002) Influence of the Temperature on the Properties of Sputtered Titanium Oxide Films. *Materials Chemistry and Physics*, **77**, 903-911. [http://dx.doi.org/10.1016/S0254-0584\(02\)00189-X](http://dx.doi.org/10.1016/S0254-0584(02)00189-X)